Inorganic Chemistry
Article

Inorg. Chem. **2009**, *48*, 8955–8964 **8955**
DOI: 10.1021/ic9014306

Dimethylammonium Hexanoate Stabilized Rhodium(0) Nanoclusters Identified as True Heterogeneous Catalysts with the Highest Observed Activity in the Dehydrogenation of Dimethylamine−Borane

Mehmet Zahmakiran and Saim Özkar*

Department of Chemistry, Middle East Technical University, 06531 Ankara, Turkey

Received July 21, 2009

Herein we report the discovery of a superior dimethylamine−borane dehydrogenation catalyst, more active than the prior best heterogeneous catalyst (Jaska, C. A.; Manners, I. *J. Am. Chem. Soc.* **2004**, *126*, 9776) reported to date for the dehydrogenation of dimethylamine−borane. The new catalyst system consists of rhodium(0) nanoclusters stabilized by $C_5H_{11}COO^-$ anions and $Me_2H_2N^+$ cations and can reproducibly be formed from the reduction of rhodium(II) hexanoate during dehydrogenation of dimethylamine−borane at room temperature. Rhodium(0) nanoclusters in an average particle size of 1.9 ± 0.6 nm $Rh(0)_{\sim 190}$ nanoclusters) provide 1040 turnovers over 26 h with a record *initial* turnover frequency (TOF) of 60 h^{-1} (the *average* TOF value is 40 h^{-1}) in the dehydrogenation of dimethylamine−borane, yielding 100% of the cyclic product $(Me_2NBH_2)_2$ at room temperature. The work reported here also includes the full experimental details of the following major components: (i) Characterization of dimethylammonium hexanoate stabilized rhodium(0) nanoclusters by using TEM, STEM, EDX, XRD, UV−vis, XPS, FTIR, ^1H, ^{13}C, and ^{11}B NMR spectroscopy, and elemental analysis. (ii) Collection of a wealth of previously unavailable kinetic data to determine the rate law and activation parameters for catalytic dehydrogenation of dimethylamine−borane. (iii) Monitoring of the formation kinetics of the rhodium(0) nanoclusters by a fast dimethylamine−borane dehydrogenation catalytic reporter reaction (Watzky, M. A.; Finke, R. G. *J. Am. Chem. Soc.* **1997**, *119*, 10382) at various $[Me_2NH\cdot BH_3]/[Rh]$ ratios and temperatures. Significantly, sigmoidal kinetics of catalyst formation was found to be well fit to the two-step, slow nucleation and then autocatalytic surface growth mechanism, A → B (rate constant k_1) and A + B → 2B (rate constant k_2), in which A is $[Rh(C_5H_{11}CO_2)_2]_2$ and B is the growing, catalytically active rhodium(0) nanoclusters. (iv) Mercury(0) and CS_2 poisoning and nanofiltration experiments to determine whether the dehydrogenation of dimethylamine−borane catalyzed by the dimethylammonium hexanoate stabilized rhodium(0) nanoclusters is homogeneous or heterogeneous catalysis.

Introduction

For the past decade, there has been growing interest in the development of transition-metal-catalyzed dehydrocoupling reactions that led to the formation of homonuclear or heteronuclear bonds between the main-group elements.[1] Among these reactions, the catalytic dehydrocoupling of amine−borane adducts has become increasingly important from the perspective of current interest in hydrogen storage,[2] because the efficient storage of hydrogen is still one of the key issues in the "Hydrogen Economy".[3] Moreover, the application of catalytic dehydrocoupling of amine−borane adducts in polymer synthesis,[4] materials science,[5] tandem dehydrogenation−hydrogenation[6] and transfer

*To whom correspondence should be addressed. E-mail: sozkar@metu.edu.tr.

(1) (a) Gauvin, F.; Harrod, F.; Woo, H. G. *Adv. Organomet. Chem.* **1998**, *42*, 363. (b) Reichl, J. A.; Berry, D. H. *Adv. Organomet. Chem.* **1998**, *43*, 197. (c) Tilley, T. D. *Acc. Chem. Res.* **1993**, *26*, 22. (d) Bartolescott, A.; Manners, I. *Dalton Trans.* **2003**, 4015. (e) Douglas, T. M.; Chaplin, A. B.; Weller, A. S. *J. Am. Chem. Soc.* **2008**, *130*, 14432.

(2) (a) Bluhm, M. E.; Bradley, M. G.; Butterick, R.; Kusari, U.; Sneddon, L. G. *J. Am. Chem. Soc.* **2006**, *128*, 7748. (b) Blaquiere, N.; Diallo-Garcia, S.; Gorelsky, S. I.; Black, D. A.; Fagnou, K. *J. Am. Chem. Soc.* **2008**, *130*, 14034. (c) Käss, M.; Friedrich, A.; Dress, M.; Schneider, S. *Angew. Chem., Int. Ed.* **2009**, *48*, 905.

(3) (a) Berg, A. W. C. V.; Arean, C. O. *Chem. Commun.* **2008**, 668. (b) Basic Research Needs for the Hydrogen Economy. Report of the Basic Energy Sciences Workshop on Hydrogen Production, Storage and Use, 2003, Office of Science, U.S. Department of Energy, www.sc.doe.gov/bes/hydrogen.pdf; (c) Annual Energy Outlook 2005 with Projections to 2025, Energy Information Administration, Feb 2005, www.eia.doe.gov/oiaf/aeo/pdf/0383(2005).pdf; (d) Turner, J.; Sverdrup, G.; Mann, K.; Maness, P. G.; Kroposki, B.; Ghirardi, M.; Evans, R. J.; Blake, D. *Int. J. Energy Res.* **2007**, *32*, 379.

(4) (a) Clark, J. T.; Lee, K.; Manners, I. *Chem. Eur. J.* **2006**, *12*, 8634. (b) Staubitz, A.; Soto, P. A.; Manners, I. *Angew. Chem.* **2008**, *120*, 6308.

(5) (a) Dorn, H.; Rodezno, J. M.; Brunnhöfer, B.; Rivard, E.; Massey, J. A.; Manners, I. *Macromolecules* **2003**, *36*, 291. (b) Jacquemin, D.; Lambert, C.; Perpete, E. A. *Macromolecules* **2004**, *37*, 1009.

(6) (a) Jaska, C. A.; Manners, I. *J. Am. Chem. Soc.* **2004**, *126*, 2698. (b) Couturier, M.; Andresena, B. M.; Tuckera, J. L.; Dubéa, P.; Breneka, S. J.; Negria, J. T. *Tetrahedron Lett.* **2001**, *42*, 2763.

Published on Web 08/24/2009

hydrogenation[7] has also made a significant contribution to the rapid development in this field. Of particular importance are the results of recent studies showing that the catalytic dehydrogenation of dimethylamine−borane ($Me_2NH \cdot BH_3$, DMAB) can be performed in the presence of a suitable catalyst under mild conditions (eq 1).[8,9]

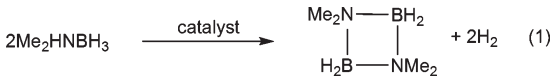

Many transition-metal catalysts such as complexes of rhodium,[10−12] iridium,[9] ruthenium,[9] palladium,[9] zirconium,[13] titanium,[13,14] and rhenium,[7] supported palladium (Pd/C)[9] and rhodium (Rh/Al_2O_3),[11] and (Oct_4N)Cl-stabilized rhodium(0) nanoclusters[11] have been tested in the dehydrogenation of DMAB. A literature search for the most active prior catalyst in the dehydrogenation of DMAB at ≤25 °C gives Chirik's important report on a previously unprecedented turnover frequency (TOF) of 420 h^{-1} at 23 °C for homogeneous catalysis using the precursor complex $[\eta^5\text{-}C_5H_3\text{-}1,3\text{-}(SiMe_3)_2)_2Ti]_2$ ($\mu_2,\eta^1,\eta^1\text{-}N_2$).[13] Unfortunately, the lifetime of the homogeneous catalyst has not been reported and, consequently, it is not known for how long the TOF would retain such a high value. Besides, the preparation of the precursor complex requires an intricate and time-consuming procedure and, most importantly, generates problems in the isolation of the dehydrogenation product from the catalyst due to homogeneous nature of the catalyst. At this concern, because of the advantages of heterogeneous catalysis[15] including simple product separation and catalyst recovery, current research has been directed toward the development of heterogeneous catalysts possessing high activity. However, a few of them provide high activity for the dehydrogenation of DMAB.[11] Among the heterogeneous catalysts tested in the dehydrogenation of DMAB (see Table 2, vide infra), the colloidal rhodium(0), in situ formed from the reduction of $[Rh(\mu\text{-}Cl)(1,5\text{-}cod)]_2$,[9,11] has been shown to provide the highest activity (TOF ≈ 10 h^{-1} at 25 °C).[11,16,17] However, the sole stabilizer present in the system is the weakly coordinating chloride anion and the dimethylammonium cation. Chloride cannot provide enough stabilization for the rhodium(0) nanoclusters, not unexpectedly, based on a previous study ranking the anions in the order of their ability to stabilize iridium(0) nanoclusters, whereby the chloride anion has been found to be the weakest stabilizer.[18] Expectedly, colloidal rhodium(0) has been observed to aggregate to bulk metal during the dehydrogenation of DMAB.[11] Nevertheless, this study[11] has clearly shown that (i) reducing the particle size of the heterogeneous catalyst provides a significant increase in its activity in the dehydrogenation of DMAB too because the fraction of surface atoms increases with the decreasing particle size[19] and (ii) transition-metal nanoparticles need to be stabilized to a certain extent in their catalytic applications.[20]

Herein we report that rhodium(0) nanoclusters, stabilized by dimethylammonium hexanoate in toluene, are the most active and long-lived catalyst in the dehydrogenation of DMAB at 25 °C. Furthermore, dimethylammonium hexanoate stabilized rhodium(0) nanoclusters were found to be the true heterogeneous catalyst, unlike the results of Jaska and Manners' work,[11] in which bulk rhodium was found to be a kinetically competent catalyst. On that account, to the best of our knowledge, this is the first example of a transition-metal nanoclusters catalyzed dehydrogenation of DMAB. Our rhodium(0) nanoclusters can reproducibly be formed in situ from the reduction of rhodium(II) hexanoate, $[(C_5H_{11}CO_2)_2Rh]_2$, during the dehydrogenation of DMAB. The reduction of the rhodium(II) precursor complex to rhodium(0) by DMAB yields 2 equiv of dimethylammonium hexanoate, $[Me_2H_2N]^+[C_5H_{11}COO]^-$ per rhodium(II) reduced to rhodium(0); the result is a highly efficient dehydrogenation catalyst for DMAB at room temperature. This new catalyst was characterized by elemental analysis, transmission electron microscopy (TEM), scanning TEM (STEM), energy-dispersive X-ray (EDX), X-ray diffraction (XRD), X-ray photoelectron spectroscopy (XPS), Fourier transform IR (FTIR), UV−vis, and ^1H, ^{13}C, and ^{11}B NMR spectroscopy.

Experimental Section

Materials. All commercially obtained compounds were used as received unless indicated otherwise: rhodium(II) hexanoate, dimethylamine−borane, carbon disulfide, and toluene were purchased from Sigma-Aldrich. Mercury (99.9%) was purchased from Atalar Chem. Ind. Toluene and methanol were distilled over sodium and magnesium, respectively, and stored in a nitrogen-atmosphere drybox. Dimethylamine−borane was purified by sublimation at 25 °C. Deuterated NMR solvents chloroform-*d* and toluene-d_8 (from Sigma-Aldrich) were transferred into the drybox for NMR sample preparations therein.

Analytical Procedures and Equipment. All reactions and manipulations were performed under an atmosphere of dry nitrogen using standard Schlenk techniques or in a Labsconco glovebox (<1 ppm oxygen) filled with dry nitrogen unless otherwise specified. The XPS analysis was performed on a Physical Electronics 5800 spectrometer equipped with a hemispherical analyzer and using monochromatic Al Kα radiation (1486.6 eV, with the X-ray tube working at 15 kV and 350 W and a pass energy of 23.5 keV). UV−vis electronic absorption spectra were recorded on a Varian Cary 5000 UV−vis−NIR spectrophotometer. The XRD pattern was recorded on a MAC Science MXP 3TZ diffractometer using Cu Kα radiation (wavelength 1.5406 Å, 40 kV, 55 mA). FTIR spectra were taken from KBr pellets using a Nicolet Magna-IR 750 spectrometer with *Omnic* software. NMR spectra were recorded on Bruker

(7) Jiang, Y.; Berke, H. *Chem. Commun.* **2007**, 3571.
(8) Jaska, C. A.; Temple, K.; Lough, A. J.; Manners, I. *Chem. Commun.* **2001**, 962.
(9) Jaska, C. A.; Temple, K.; Lough, A. J.; Manners, I. *J. Am. Chem. Soc.* **2003**, *125*, 9424.
(10) Chen, Y.; Fulton, J. L.; Linehan, J. C.; Autrey, T. *J. Am. Chem. Soc.* **2005**, *127*, 3254.
(11) Jaska, C. A.; Manners, I. *J. Am. Chem. Soc.* **2004**, *126*, 9776.
(12) Sloan, M.; Clark, T. J.; Manners, I. *Inorg. Chem.* **2009**, *48*, 2429.
(13) Pun, D.; Lobkovsky, E.; Chirik, P. J. *Chem. Commun.* **2007**, 3297.
(14) Clark, T. J.; Russell, C. A.; Manners, I. *J. Am. Chem. Soc.* **2006**, *128*, 9582.
(15) Thomas, J. M.; Thomas, W. J. *Principles and Practice of Heterogeneous Catalysis*; VCH: New York, 1997.
(16) The TOF value has not been reported for the rhodium(0) colloid catalyzed dehydrogenation of DMAB in the respective article[9] but can be estimated from the data given: Complete dehydrogenation has been achieved by using a $[Rh(\mu\text{-}Cl)(1,5\text{-}cod)]_2$ catalyst of 2 mol % rhodium at 25 °C in ca. 8 h.[11]
(17) Unfortunately, in none of these studies has the very important catalysis parameter catalytic lifetime (i.e., total turnovers, TTO) been reported for the dehydrogenation of DMAB.
(18) Özkar, S.; Finke, R. G. *J. Am. Chem. Soc.* **2002**, *124*, 5796.
(19) Pool, R. *Science* **1990**, *248*, 1186.
(20) Özkar, S.; Finke, R. G. *Langmuir* **2002**, *18*, 7653.

Avance DPX 400 MHz spectrometer (400.1 MHz for ^{1}H NMR; 100.6 MHz for ^{13}C NMR; 128.2 MHz for ^{11}B NMR). Tetramethylsilane was used as the internal reference for ^{1}H and ^{13}C NMR chemical shifts. $BF_3 \cdot (C_2H_5)_2O$ was used as the external reference for ^{11}B NMR chemical shifts. TEM, STEM, and EDX analyses were done on a FEI Tecnai G^2 (X-Twin) microscope with an accelerating voltage of 120 kV (2 Å resolution).

General Procedure for Rhodium(0) Nanocluster Formation and Determination of Their Catalytic Activity in the Dehydrogenation of Dimethylamine−Borane. The in situ formation of rhodium(0) nanoclusters and the concomitant dehydrogenation of DMAB were performed in a Fischer−Porter (F−P) pressure bottle connected to a line through Swagelock tetrafluoroethylene (TFE)-sealed quick connects and to an Omega PX-302 pressure transducer interfaced through an Omega D1131 digital transmitter to a computer using the RS-232 module as described elsewhere.[21] The progress of an individual dehydrogenation reaction was followed by monitoring the increase in the pressure of H_2 gas on the *LabVIEW 8.0* program. The catalytic activity of rhodium(0) nanoclusters was determined by measuring the rate of hydrogen generation. A stock solution of rhodium(II) hexanoate with [Rh] = 5.0 mM was prepared by dissolving 0.0625 mmol (43 mg, 0.125 mmol of Rh) of $[(C_5H_{11}CO_2)_2Rh]_2$ in 25 mL of toluene in a Schlenk tube by gentle warming. In a typical experiment, 60.7 mg (1.0 mmol) of DMAB was weighed and dissolved in 8 mL of toluene added via a 10 mL gastight syringe to yield a clear colorless solution. The solution was then transferred via a disposable glass pipet into a new 22 × 175 mm pyrex culture tube containing a new $^5/_{16}$ in. × $^5/_8$ in. Teflon-coated magnetic stir bar. The culture tube was then sealed inside the F−P bottle, which was brought outside the drybox and placed inside a constant-temperature circulating water bath thermostated at 25.0 ± 0.1 °C unless otherwise specified. Next, the F−P bottle was connected to the line, which had already been evacuated for at least 30 min to remove any trace of oxygen and water present, via its Swagelock TFE-sealed quick connects. Under nitrogen purging (14 mL of dry nitrogen/s), 2.0 mL of a stock solution of rhodium(II) hexanoate was added to the F−P bottle rapidly via tap of bottle by using a 10 mL pyrex volumetric pipet, which had been nitrogen-flushed three times. When a constant pressure inside the F−P bottle was established, the reaction was started (t = 0 min) by stirring the mixture at 900 rpm. When no more hydrogen generation was observed, the experiment was stopped, the F−P bottle was sealed and disconnected from the line, and the hydrogen pressure was released. Then the F−P bottle was transferred back into the drybox. An approximately 0.5 mL aliquot of the reaction solution in the culture tube was withdrawn with a 9 in. glass Pasteur pipet and added to 1 g of $CDCl_3$ in an individual glass ampule. The solution was then transferred into a quartz NMR sample tube (Norell S-500-QTZ), which was subsequently sealed and then brought out of the drybox. The ^{11}B NMR spectrum of this solution showed that $Me_2NH \cdot BH_3$ at −14 ppm (q, J_{B-H} = 95 Hz) is completely converted to $[Me_2NBH_2]_2$ at 5 ppm (t, J_{B-H} = 112 Hz).

Data Handling and Curve Fit of Hydrogen Generation Data. The raw pressure versus time data collected with the computer-interfaced transducer were exported from *LabVIEW 8.0* and imported into *OriginPro 8*. Before any fitting was done, the raw data from experiments carried out in toluene were corrected for the buildup of pressure in the F−P bottle due to the solvent vapor pressure and the initial nitrogen pressure was then converted into the values in proper units, volume of hydrogen (mL). Curve fitting of the volume of hydrogen (mL) (or, equivalently, loss in [DMAB]) versus time data to the Finke−Watzky two-step mechanism was performed as described elsewhere[22] using the software package *OriginPro 8*, which is a nonlinear regression subroutine and uses a modified Levenberg−Marquardt algorithm.[23]

All of the catalytic dehydrogenation experiments were performed in a manner similar to that described above. The details of separate experiments are given in the Supporting Information.

Results and Discussion

In Situ Formation of Rhodium(0) Nanoclusters during the Dehydrogenation of Dimethylamine−Borane and Identification of Rhodium(0) Nanoclusters as the True Soluble Heterogeneous Catalyst in the Dehydrogenation of Dimethylamine−Borane. i. Kinetic Evidence for Rhodium(0) Nanocluster Formation. The progress of rhodium(0) nanocluster formation and concomitant dehydrogenation of dimethylamine−borane was followed by monitoring the changes in hydrogen pressure, which was then converted into the equivalent concentration loss of DMAB, using the known 1:1 H_2/DMAB stoichiometry (eq 1). Figure 1 shows the DMAB loss versus time plot for the dehydrogenation of DMAB starting with a $[(C_5H_{11}CO_2)_2Rh]_2$ precatalyst in toluene at 25 ± 0.1 °C. The formation kinetics of the $Rh(0)_n$ nanocluster catalyst can be obtained using DMAB dehydrogenation as the reporter reaction,[22,24,25] (Scheme 1), in which A is the added precursor $[(C_5H_{11}CO_2)_2Rh]_2$ and B is the growing $Rh(0)_n$ nanocluster. The dehydrogenation of DMAB will accurately report on and amplify the amount of $Rh(0)_n$ nanocluster catalyst, B, present if the dehydrogenation rate is fast in comparison to the rate of nanocluster formation. It was shown that the dehydrogenation is zero-order in [DMAB] (vide infra) to ensure that the dehydrogenation reporter reaction is fast relative to the rate of slower nanocluster formation k_1 and k_2 steps (Scheme 1). Sigmoidal kinetics can be seen in Figure 1, just as an example of all of the data collected under different conditions (see later), and fit well by the Finke−Watzky two-step nucleation and autocatalytic growth mechanism of nanocluster formation.[22] The observation of a sigmoidal dehydrogenation curve and its curve fit to the slow, continuous nucleation A → B (rate constant k_1) followed by autocatalytic surface growth A + B → 2B (rate constant k_2) kinetics is very strong evidence for the formation of a metal(0) nanocluster catalyst from a soluble transition-metal complex in the presence of a reducing agent.[22] The rate constants determined from the nonlinear least-squares curve fit in Figure 1 are $k_1 = 2.13 \times 10^{-3}$ min^{-1} and $k_2 = 36$ M^{-1} min^{-1} (the mathematically required correction has been made to k_2 for the stoichiometry factor of 100, as described elsewhere,[24] but not for the "scaling factor"; that is, no correction has been made for the changing number of Rh atoms on the growing metal surface).[24]

ii. UV−Vis Electronic Absorption Spectroscopy and TEM Studies Demonstrating the In Situ Formation of

(21) (a) Zahmakiran, M.; Özkar, S. *Langmuir* **2008**, *24*, 7065. (b) Zahmakiran, M.; Özkar, S. *Langmuir* **2009**, *25*, 2667.

(22) (a) Watzky, M. A.; Finke, R. G. *J. Am. Chem. Soc.* **1997**, *119*, 10382. (b) Watzky, M. A.; Finke, R. G. *Chem. Mater.* **1997**, *9*, 3083.

(23) Press, W. H.; Flannery, B. P.; Teukolsky, S. A.; Vetterling, W. T. *Numerical Recipies*; Cambridge University Press: Cambridge, U.K., 1989.

(24) Widegren, J. A.; Aiken, J. D.; Özkar, S.; Finke, R. G. *Chem. Mater.* **2001**, *13*, 312.

(25) Widegren, J. A.; Bennett, M. A.; Finke, R. G. *J. Am. Chem. Soc.* **2003**, *125*, 10301.

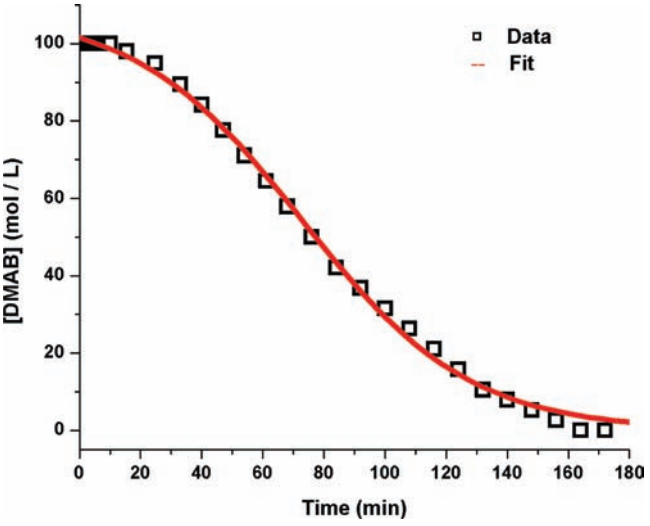

Figure 1. Plot of [DMAB] loss vs time for the dehydrogenation of DMAB starting with 0.005 mmol of $[(C_5H_{11}CO_2)_2Rh]_2$ and 1 mmol of $Me_2NH\cdot BH_3$ in 10 mL of toluene at 25 ± 0.1 °C. The sigmoidal curve fits well to the two-step mechanism for the rhodium(0) nanocluster formation.[22]

Scheme 1. Illustration of the Dehydrogenation of Dimethylamine−Borane as the Reporter Reaction

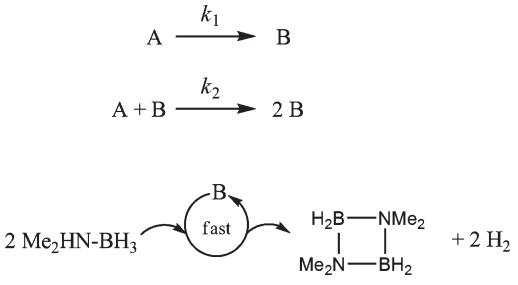

A is the precursor $[(C_5H_{11}CO_2)_2Rh]_2$, and B is the growing $Rh(0)_n$ nanocluster.

Rhodium(0) Nanoclusters. During the reduction of the precursor rhodium(II) complex to rhodium(0), the reaction solution gradually changed its color from green to pink, to reddish brown, to brown, and ultimately to dark brown at room temperature. This color change reflects the reduction of Rh^{2+} to Rh^0 through Rh^+. Monitoring the UV−vis electronic absorption spectra of the solution provides a convenient way to follow this conversion. The starting solution of $[(C_5H_{11}CO_2)_2Rh]_2$ exhibits three absorption bands at λ_{max} = 305, 428, and 699 nm in the spectrum. When these are compared to the literature values,[26] the bands at 428 and 699 nm are attributed to the d−d transitions and the strong band at 305 nm to the ligand-to-metal charge-transfer transition in $[(C_5H_{11}CO_2)_2Rh]_2$. The spectral feature changes immediately when DMAB is added to the solution, and a new band grows at λ_{max} = 526 nm, which can be assigned to the d−d transition in a rhodium(I) species by comparison with the literature values for rhodium(I) complexes,[27] and loses intensity during the course of the reaction. After 35 min of reaction (about 10% conversion of DMAB), the UV−vis spectrum of the solution exhibits a continuous absorption characteristic for rhodium(0) nanoclusters because of the surface plasmon resonance, with a steep rise in absorbance at short wavelengths.[28] This observation indicates that the reduction of Rh^{2+} to Rh^0 is complete when only 10% DMAB is dehydrogenated.

The electron microscopy study on the rhodium(0) nanoclusters was started by taking the TEM image of a solution of the precursor complex, $[(C_5H_{11}CO_2)_2Rh]_2$, by considering the crucial result of Manners' group,[11] reporting that even a 70 kV TEM beam induces rhodium(0) nanocluster formation from a $[(1,5\text{-COD})RhCl]_2$ precatalyst.[11] The formation of rhodium(0) nanoclusters from the reduction of the precursor under an electron beam has also been verified by Finke et al.[29] A low-resolution TEM image of the $[(C_5H_{11}CO_2)_2Rh]_2$ precursor depicts the presence of only micrometer-sized particles even the sample was exposed to a 120 kV electron beam over 10 min (Figure 2a). However, under the same conditions (V_{acc} = 120 kV; $t_{exposure}$ = 10 min), a low-resolution TEM image of the sample harvested from the solution after 35 min in the dehydrogenation reaction started with DMAB and $[(C_5H_{11}CO_2)_2Rh]_2$ in toluene shows only the presence of rhodium(0) nanoclusters. The mean particle size of rhodium(0) nanoclusters was found to be 1.9 ± 0.6 nm ($Rh(0)_{\sim 190}$ nanoclusters)[30] as measured from the TEM image given in Figure 2c by using an NIH image program,[31] whereby 470 nontouching particles were counted. A TEM image of the sample harvested after the complete dehydrogenation of DMAB (3 h) in Figure 2d shows that the particle size of rhodium(0) nanoclusters is slightly increased to the average value of 2.3 ± 0.8 nm ($Rh(0)_{\sim 460}$ nanoclusters),[30] whereby 350 nontouching particles were counted. STEM-EDX analyses (vide infra) confirm the presence of rhodium in the sample.[32] These results reveal that rhodium(0) nanoclusters are formed as the primary reaction product and the dehydrogenation of DMAB is a heterogeneous catalysis involving rhodium(0) nanoclusters.

iii. Mercury(0) and CS_2 Poisoning. The ability of mercury(0) to poison heterogeneous metal(0) catalysts,[33] by amalgamating the metal catalyst or being adsorbed on its surface has been known for a long time; this is the single most widely used test of homogeneous versus heterogeneous catalysis.[34] The suppression of catalysis by mercury(0) is considered to be compelling evidence for a heterogeneous catalysis. After about 40% conversion in

(26) Stranger, R.; Medley, A. G.; McGrady, J. E.; Garrett, J. M.; Appleton, T. G. *Inorg. Chem.* **1996**, *35*, 2268 and references cited therein.
(27) (a) Setsune, J. I.; Yamauchi, T.; Tanikawa, S. *Chem. Lett.* **2002**, *31*, 188. (b) Moszne, M. *Inorg. Chim. Acta* **2004**, *357*, 3613.
(28) Creighton, J. A.; Eadon, D. G. *J. Chem. Soc., Faraday Trans.* **1991**, *87*, 3881.
(29) Hagen, M. C.; Widegren, A. J.; Maitlis, P. M.; Finke, R. G. *J. Am. Chem. Soc.* **2005**, *127*, 4423.
(30) Using the equation $N = N_0pV/102.9$, where $N_0 = 6.022 \times 10^{23}$, p = 12.5 g/cm^3, and $V = (4/3)\pi(D/2)^3$, the number of metal atoms in the spherical 1.9 and 2.3 nm rhodium(0) nanoclusters were estimated to be 190 and 460, respectively.
(31) Hutchison, J. E.; Woehrle, G. H.; Özkar, S.; Finke, R. G. *Turkish J. Chem.* **2006**, *30*, 1.
(32) Jones, I. P. *Chemical Microanalysis Using Electron Beams*; The Institute of Materials: London, 1992.
(33) Whitesides, G. M.; Hackett, M.; Brainard, R. L.; Lavalleye, J. P.; Sowinski, A. F.; Izumi, A. N.; Moore, S. S.; Brown, D. W.; Staudt, E. M. *Organometallics* **1985**, *4*, 1819.
(34) Widegren, J. A.; Finke, R. G. *J. Mol. Catal. A: Chem.* **2003**, *198*, 317.

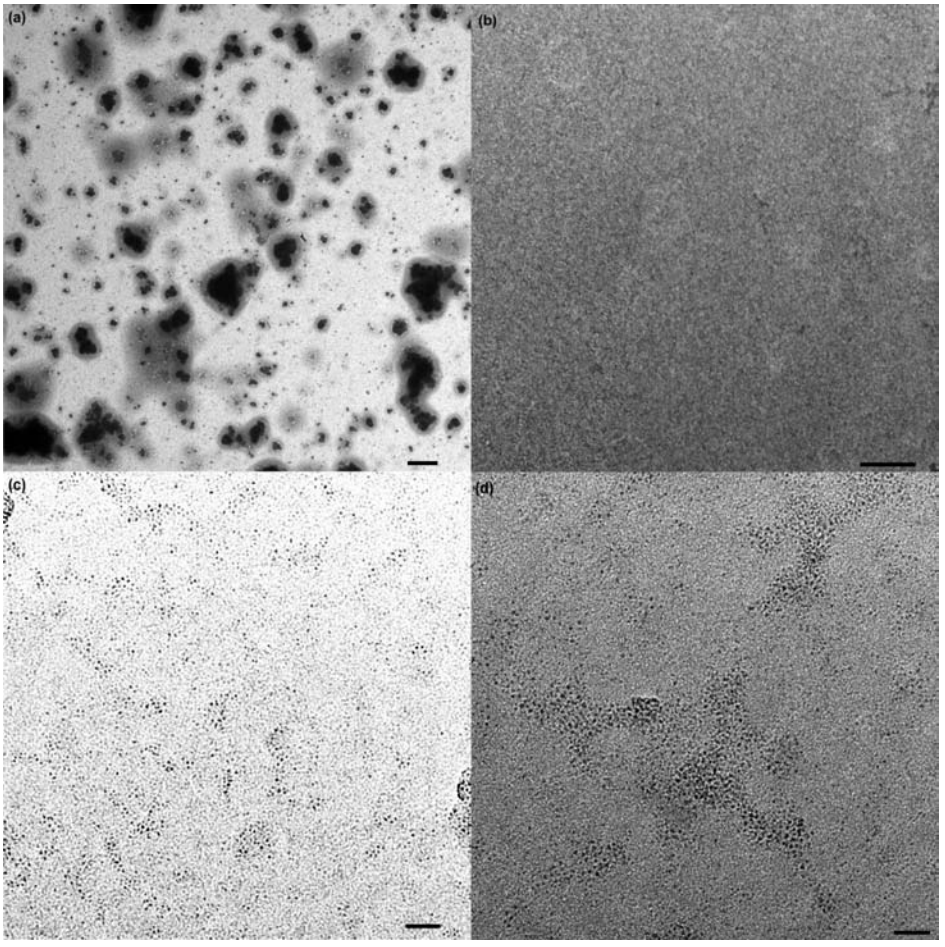

Figure 2. (a) Low-resolution TEM image of $[(C_5H_{11}CO_2)_2Rh]_2$ indicating the existence of micrometer-sized particles (the scale bar represents 2 μm). (b) Low-resolution TEM image of the reaction mixture (0.005 mmol of $[(C_5H_{11}CO_2)_2Rh]_2$ + 1 mmol of $Me_2NH \cdot BH_3$; the scale bar represents 1 μm) and TEM images of the same reaction mixture harvested after (c) 10% conversion of DMAB showing 1.9 ± 0.6 nm rhodium(0) nanoclusters (470 counted) (the scale bar represents 20 nm). (d) Complete conversion of DMAB showing 2.3 ± 0.8 nm rhodium(0) nanoclusters (350 counted) (the scale bar represents 10 nm).

a typical dehydrogenation experiment, 180 equiv of mercury per rhodium was added into the reaction solution and the progress of the reaction was followed by monitoring the hydrogen pressure, as shown in Figure 3. The catalytic dehydrogenation of DMAB was ceased completely upon mercury addition. A control experiment performed starting with the same amounts of DMAB and $[(C_5H_{11}CO_2)_2Rh]_2$, which has been pretreated with mercury, shows the same catalytic activity as the one observed without treatment in the dehydrogenation of DMAB, indicating that mercury does not react with the precursor $[(C_5H_{11}CO_2)_2Rh]_2$. In a separate experiment, the same protocol as described in mercury poisoning was carried out, but 0.1 equiv of CS_2 per rhodium was used instead of elemental mercury. As shown in Figure 3, the addition of 0.1 equiv of CS_2 completely impedes the catalytic dehydrogenation of DMAB.[35,36] The observation that the addition of $\ll 1$ equiv of CS_2 per rhodium stops the reaction is compelling evidence for heterogeneous catalysis.[34] The logic here is that in a heterogeneous catalyst only a fraction of the metal atoms is on the surface (e.g., about 60% of the rhodium is on the surface of a 1.9 nm $Rh(0)_{\sim 190}$ nanocluster). Experimentally, a minimum CS_2/total rhodium ratio of 0.019 for complete poisoning of the

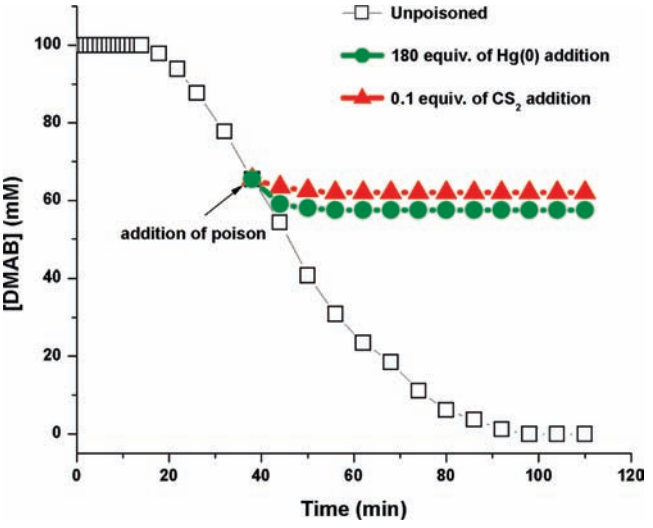

Figure 3. Plot of [DMAB] vs time for mercury(0) and CS_2 poisoning experiments starting with 0.015 mmol of $[(C_5H_{11}CO_2)_2Rh]_2$ and 1 mmol of $Me_2NH \cdot BH_3$ in 10 mL of toluene at 25 ± 0.1 °C and after the addition of 180 equiv of mercury(0) or 0.1 equiv of CS_2 when about 40% conversion was achieved in separate experiments.

(35) Hornstein, B. J.; Aiken, J. D.; Finke, R. G. *Inorg. Chem.* **2002**, *41*, 1625.
(36) Vargaftik, M. N.; Zargorodnikov, V. P.; Stolarov, I. P.; Moiseev, I. I.; Kochubey, D. I.; Likholobov, V. A.; Chuvilin, A. L.; Zamaracv, K. I. *J. Mol. Catal.* **1989**, *53*, 315.

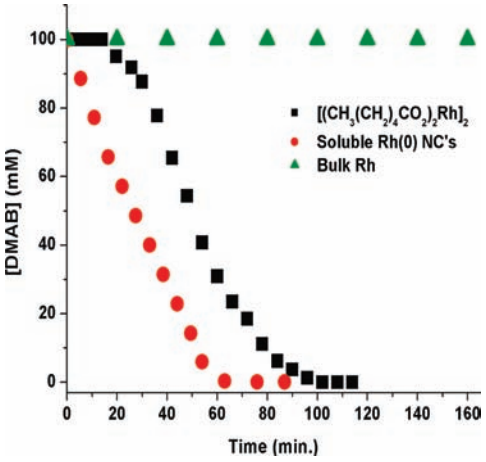

Figure 4. Plots of [DMAB] loss vs time for three separate dehydrogenation experiments: (■) dehydrogenation of DMAB starting with 0.015 mmol of $[(C_5H_{11}CO_2)_2Rh]_2$ and 1 mmol of $Me_2NH\cdot BH_3$ in 10 mL of toluene; (red ●) dehydrogenation of DMAB starting with the filtrate obtained from filtration of a brown solution after the first run of dehydrogenation; (green ▲) dehydrogenation starting with the black bulk metal obtained from filtration after the first run of dehydrogenation.

rhodium(0) nanoclusters was determined by performing a series of experiments with CS_2 in various concentrations.[37]

iv. Kinetic Competence of the Soluble Rhodium(0) Nanoclusters, Not the Bulk Rhodium(0) Metal. Two separate experiments were performed to determine which of the following is responsible for the observed catalysis: (i) the soluble rhodium(0) nanoclusters formed in situ during the dehydrogenation, (ii) the black bulk rhodium metal that becomes visible to the naked eye after 6 h, or conceivably (iii) some combination of (i) and (ii). First, the dark-brown reaction solution formed at the end of the dehydrogenation of DMAB was filtered through a micropore filter to remove any traces of bulk metal (but not the nanoclusters). Then the catalytic activity of the filtrate was tested in the dehydrogenation of DMAB by the addition of a fresh substrate. In such an experiment, the dehydrogenation of DMAB was observed to start immediately without an induction time (Figure 4) and at a rate kinetically competent to account for the observed dehydrogenation. Next, the catalytic activity of the bulk metal isolated after the first run was tested by the addition of fresh DMAB. The bulk metal showed no activity within the same period of time in the dehydrogenation of DMAB (Figure 4). These results indicate that the rhodium(0) nanoclusters formed in situ during the dehydrogenation of DMAB are the true kinetically competent catalyst.[38]

Further Characterization of Rhodium(0) Nanoclusters and Identification of Dimethylammonium Hexanoate as the Stabilizer for Rhodium(0) Nanoclusters Formed In Situ during the Dehydrogenation of Dimethylamine−Borane. The ^{11}B NMR spectrum taken from the reaction solution at the end of the dehydrogenation of DMAB (when no more hydrogen is evolved) shows that $Me_2NH\cdot BH_3$ ($\delta = -14$ ppm, q) is completely converted to the cyclic product $[Me_2NBH_2]_2$ ($\delta = 5$ ppm, t).[6−14] The rhodium(0) nanoclusters were isolated from the reaction solution as black powders by successive centrifugation followed by vacuum drying, all under a nitrogen atmosphere, and analyzed by using FTIR, XRD, and XPS. The powder XRD pattern of this bulk material exhibits a distinct reflection at a 2θ value of 40.8° and can be unequivocally ascribed to the (111) reflection of metallic rhodium.[39] Thus, on the basis of XRD analysis, it can be concluded that the reduction of $[(C_5H_{11}CO_2)_2Rh]_2$ with DMAB leads to the formation of rhodium(0) metal. Additionally, the XPS of the same sample provides evidence supporting the oxidation state of rhodium and the surface composition. The main peaks observed in the survey scan XPS are C 1s, Rh $3d_{5/2}$, Rh $3d_{3/2}$, N 1s, and O 1s at 285, 305, 310, 399, and 540 eV, respectively. The Rh 3d XPS spectrum of the rhodium(0) nanoclusters fits well to two peaks at 305.2 and 310.6 eV, readily assigned to Rh(0) $3d_{5/2}$ and Rh(0) $3d_{3/2}$, respectively.[40]

FTIR spectrum of this bulk material shows two strong absorption bands at 1360 and 1440 cm^{-1} due the symmetric and asymmetric stretching of the carboxylate group in addition to the bands for CH and NH stretching, indicating the presence of a hexanoate anion and a dimethylammonium cation.[41,42] The observation of two absorption bands for the carboxylate group with a separation of 80 cm^{-1}, much smaller than those of ionic complexes (164−171 cm^{-1}), indicates that the carboxylate anions are adsorbed on the nanocluster surface as a chelating bidendate ligand.[43−45] Additionally, ^{13}C

(37) In order to determine the true number of catalytically active surface sites, we performed seven independent CS_2 poisoning experiments by changing the mole ratio of CS_2/total rhodium (Supporting Information). In each experiment, the relative signal intensity of $[Me_2N\cdot BH_2]_2$ at 5 ppm to that of $Me_2NH\cdot BH_3$ at −14 ppm in the ^{11}B NMR spectrum was used to calculate the conversion of DMAB.

(38) Conventionally, the criterion of solubility has been used to categorize "homogeneous" and "heterogeneous" catalysts. (a) Hamlin, J. E.; Hirai, K.; Millan, A.; Maitlis, P. M. *J. Mol. Catal.* **1980**, *7*, 543. (b) Whitesides, G. M.; Hackett, M.; Brainard, R. L.; Lavalleye, J. P. P. M.; Sowinski, A. F.; Izumi, A. N.; Moore, S. S.; Brown, D. W.; Staudt, E. M. *Organometallics* **1985**, *4*, 1819. (c) Anton, D. R.; Crabtree, R. H. *Organometallics* **1983**, *2*, 855. (d) Crabtree, R. H.; Mihelcic, J. M.; Quirk, J. M. *J. Am. Chem. Soc.* **1979**, *101*, 7738. (e) Collman, J. P.; Kosydar, K. M.; Bressan, M.; Lamanna, W.; Garrett, T. *J. Am. Chem. Soc.* **1984**, *106*, 2569. (f) Lewis, L. N.; Lewis, L. *J. Am. Chem. Soc.* **1996**, *108*, 7228. (g) Lewis, L. N. *J. Am. Chem. Soc.* **1990**, *112*, 5998. However, it is difficult to make this differentiation in the case of the soluble (dispersible) nanocluster catalysts involved because colloidal solutions often appear homogeneous to the eye. With this concern, for distinction of homogeneous and heterogeneous catalysis, we followed Schwartz's definition (Schwartz, J. *Acc. Chem. Res.* **1985**, *18*, 302) and Finke's methodology (Widegren, J. A.; Finke, R. G. *J. Mol. Catal. A: Chem.* **2003**, *198*, 317) stating that "Specifically, heterogeneous catalysts have multiple types of active sites and homogeneous catalysts have a single type of active site" and referring to the soluble (i.e., dispersible) rhodium(0) nanoclusters as the soluble heterogeneous catalyst.

(39) Bruss, J. A.; Gelesky, M. A.; Machado, G.; Dupont, J. *J. Mol. Catal. A: Chem.* **2006**, *252*, 212.

(40) (a) Wagner, C.; Riggs, W. M.; Davis, L. E.; Moulder, J. F.; Muilenberg, G. E. *Handbook of X-ray Photoelectron Spectroscopy*; Physical Electronic Division, Perkin-Elmer: New York, 1979; Vol. *55*, p 344. (b) Park, K. W.; Choi, J. H.; Kwon, B. K.; Lee, S. A.; Sung, Y. E.; Ha, H. Y.; Hong, S. A.; Kim, H.; Lee, S. A.; Sung, Y. A.; Ha, H. Y.; Hong, S. A.; Kim, H.; Wieckowski, A. *J. Phys. Chem. B* **2002**, *106*, 1869. (c) Zhang, X.; Chan, K. Y. *Chem. Mater.* **2003**, *15*, 451.

(41) Umumera, J.; Cameron, D. G.; Manstch, H. H. *J. Phys. Chem.* **1980**, *84*, 2272.

(42) Murphy, C. A.; Cameron, T. S.; Cooke, M. W.; Aquino, M. A. S. *Inorg. Chim. Acta* **2000**, *305*, 225.

(43) Lin, S.-J.; Hong, T.-N.; Tung, J.-Y.; Chen, J.-H. *Inorg. Chem.* **1997**, *36*, 3886.

(44) Deacon, G. B.; Phillips, R. J. *Coord. Chem. Rev.* **1980**, *33*, 227.

(45) Nakamoto, K. *Infrared and Raman Spectra of Inorganic and Coordination Compounds*, 4th ed.; John Wiley and Sons: New York, 1986.

Scheme 2. Stoichiometry for the Formation of $[Me_2H_2N^+][C_5H_{11}COO^-]$ plus a $Rh(0)_n$ Nanocluster Catalyst and the Dehydrogenation of Dimethylamine−Borane

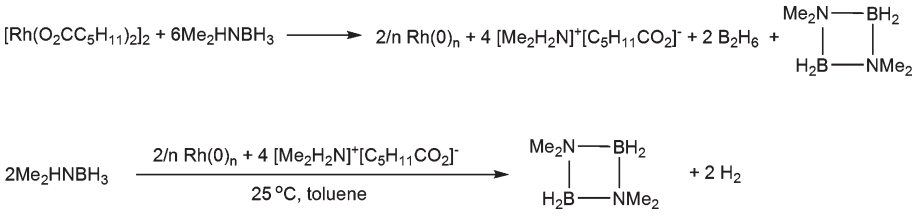

and ^{11}B NMR spectra taken from the reaction solution after a similar separate experiment, performed starting with 0.015 mmol of $[(C_5H_{11}CO_2)_2Rh]_2$ plus 0.12 mmol of $Me_2NH \cdot BH_3$ in toluene-d_8, show only the signals of $[C_5H_{11}COO^-][Me_2H_2N^+]$ and $[Me_2NBH_2]_2$. This provides compelling evidence for the identification of the reaction products. $[Me_2NBH_2]_2$ is the known product of DMAB dehydrogenation.[8,9,11] The formation of $[Me_2H_2N^+][C_5H_{11}COO^-]$ likely arises from the protonation of dimethylamine−borane[11] by hexanoic acid $C_5H_{11}COOH$, which is generated as transient from the reduction of rhodium(II) hexanoate in solution. The protonation of DMAB also releases gaseous diborane, B_2H_6, which can be trapped in dry methanol as $B(OMe)_3$ and quantified by ^{11}B NMR (see the Supporting Information). Taking all of the results together, one can conclude the in situ formation of dimethylammonium hexanoate stabilized rhodium(0) nanoclusters[46] during the dehydrogenation of DMAB (Scheme 2).

Initial Kinetic Studies and Determination of the Activation Parameters for the Catalytic Dehydrogenation of Dimethylamine−Borane. Figure 5 shows the plots of [DMAB] loss versus time for the dehydrogenation of DMAB started with different concentrations of $[(C_5H_{11}CO_2)_2Rh]_2$ in toluene at 25 ± 0.1 °C. A fast dehydrogenation starts after an induction time of 10−16 min. The dehydrogenation rate, determined from the nearly linear portion of the plots, increases with the catalyst concentration (Table 1). Plotting the dehydrogenation rate versus rhodium concentration (both on logarithmic scales) gives a straight line with a slope of 0.97 ± 0.03. That is, an apparent first-order dependence on the catalyst concentration is observed. The effect of the substrate concentration on the dehydrogenation rate was also studied by performing a series of experiments starting with variation of the initial concentration of DMAB while keeping the catalyst concentration constant at 25 ± 0.1 °C. Figure 6a shows the plots of [DMAB] loss versus time and their curve fit to the Finke−Watzky two-step mechanism[22] for the catalytic dehydrogenation of DMAB in these experiments. In a substrate concentration higher than 90 mM, the catalytic dehydrogenation of DMAB appears to be zero-order in the substrate concentration, while at lower substrate concentrations, one observes a first-order dependence (Figure 6b). The dehydrogenation of DMAB was also carried out at various temperatures in the range of 20−40 °C. The values of rate

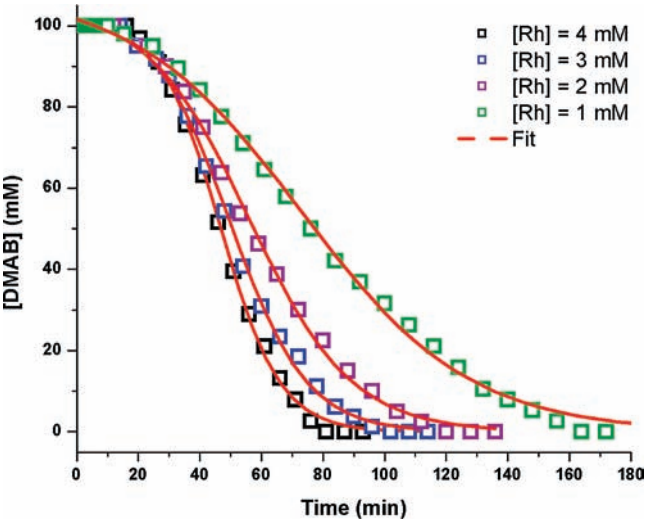

Figure 5. Plots of [DMAB] loss vs time for the dehydrogenation of DMAB started with a solution containing 100 mM $Me_2NH \bullet BH_3$ plus $[(C_5H_{11}CO_2)_2Rh]_2$ in various Rh concentrations at 25.0 ± 0.1 °C. All the data curve fit well to the 2-step mechanism for the Rh(0) nanocluster formation.[22].

constant k determined from the nearly linear portions of the [DMAB] loss versus time plots at five different temperatures (Figure 7) are used to calculate the activation parameters: activation energy $E_a = 34$ kJ/mol, activation enthalpy $\Delta H^{\ddagger} = 34.5$ kJ/mol, and activation entropy $\Delta S^{\ddagger} = -133$ J/mol·K. Note that this is the first report on the values of the activation parameters for the catalytic dehydrogenation of DMAB. The activation energy value found for the dehydrogenation catalyzed by rhodium(0) nanoclusters is slightly higher than those found for the platinum-catalyzed dehydrogenation of cyclohexene (E_a = 32 kJ/mol),[47a] the Cu^0/AlMg-catalyzed dehydrogenation of *n*-octyl alcohol (E_a = 19.5 kJ/mol),[47b] and the Pt/C-catalyzed dehydrogenation of 2-propanol (E_a = 28 kJ/mol)[47f] but lower than those found for the Pt/SiO_2-catalyzed dehydrogenation of cyclohexene (E_a = 66 kJ/mol),[47a] the Pt/Al_2O_3-catalyzed dehydrogenation of cyclohexane (E_a = 94 kJ/mol),[47c] the VO_x/Al_2O_3-catalyzed oxidative

(46) The reaction stoichiometry given in the first equation of Scheme 2 was confirmed by elemental and ICP-OES analyses and ^1H, ^{13}C, and ^{11}B NMR spectroscopies performed at the end of the reaction in which 20 mmol of $Me_2NH \cdot BH_3$ and 0.2 mmol of $[(C_5H_{11}CO_2)_2Rh]_2$ were combined and heated at 45 °C for 12 h (Supporting Information).

(47) (a) Rioux, R. M.; Hsu, B. B.; Grass, M. E.; Song, H.; Somorjai, G. A. *Catal. Lett.* **2008**, *126*, 10. (b) Crivello, M. A.; Perez, C. F.; Mendieta, S. N.; Casuscelli, S. A.; Eimer, G. A.; Elias, V. A.; Herrero, E. R. *Catal. Today* **2008**, *133*, 787. (c) Miguel, S. A.; Bocanegra, S. A.; Vilella, M. J.; Ruiz, G.; Scelza, O. A. *Catal. Lett.* **2007**, *119*, 5. (d) Frank, B.; Dinse, A.; Ovsitser, O.; Kondratenko, E. V.; Schomacker, R. *Appl. Catal. A* **2007**, *323*, 66. (e) Leruth, G. N.; Valcarcel, A.; Ramirez, J. A.; Ricart, J. M. *J. Phys. Chem. C* **2007**, *111*, 860. (f) Rioux, R. M.; Vannice, M. A. *J. Catal.* **2005**, *233*, 147. (g) Kvande, I.; Chen, D.; Ronning, M.; Venvik, H. J.; Holmen, A. *Catal. Today* **2005**, *100*, 391. (h) Ilyas, M.; Ikramullah *Catal. Commun.* **2004**, *5*, 1.

Table 1. k_1, k_2, t (Induction Time) and the Dehydrogenation Rate of Dimethylamine−Borane Depending on the [DMAB]/[Rh] Ratios and Temperature[a]

entry	$[DMAB]_0$ (mM)	$[Rh]_0$ (mM)	T (°C)	$k_1 \times 10^3$ (min^{-1})[b]	k_2 (M^{-1} min^{-1})[b,c]	$k_2/k_1 \times 10^{-3}$ (M^{-1})	induction time (min)	(TOF) (h^{-1})	rate = −d[DMAB]/dt (mM min^{-1})
1	100	1.0	25	2.13 ± 0.15	36 ± 1	1.69 ± 1.27	10	55	0.92
2	100	2.0	25	1.72 ± 0.17	35 ± 2	20.3 ± 2.32	12	50	1.64
3	100	3.0	25	1.21 ± 0.12	34 ± 3	28.0 ± 3.72	14	40	1.96
4	100	4.0	25	0.73 ± 0.08	34 ± 2	46.6 ± 5.79	16	35	2.29
5	150	2.0	25	3.61 ± 0.25	20 ± 1	5.5 ± 0.47	8	50	1.68
6	125	2.0	25	3.25 ± 0.25	23 ± 2	7.0 ± 0.82	10	50	1.63
7	90	2.0	25	2.26 ± 0.29	33 ± 1	14.6 ± 1.92	13	45	1.48
8	75	2.0	25	2.72 ± 0.04	28 ± 2	10.9 ± 0.75	14	35	1.17
9	60	2.0	25	2.71 ± 0.05	26 ± 2	9.5 ± 0.76	15	30	1.00
10	50	2.0	25	1.65 ± 0.02	37 ± 4	22.4 ± 2.44	16	26	0.86
11	100	3.0	20	0.49 ± 0.04	21 ± 3	42.8 ± 7.05	18	30	1.47
12	100	3.0	30	3.02 ± 0.36	37 ± 5	12.2 ± 2.21	9	50	2.50
13	100	3.0	35	5.05 ± 0.61	43 ± 7	8.5 ± 1.72	5	60	3.04
14	100	3.0	40	9.50 ± 1.55	72 ± 15	7.5 ± 0.53	1	80	3.96

[a] Each experiment in this table was repeated at least three times. [b] Parameter initialization in each curve fitting was achieved by 100 iterations. [c] The mathematically required correction has been made to k_2 for the stoichiometry factor of 100 as described elsewhere,[22] but not for the "scaling factor"; that is, no correction has been made for a change of the number of Rh atoms on the growing metal surface.[24]

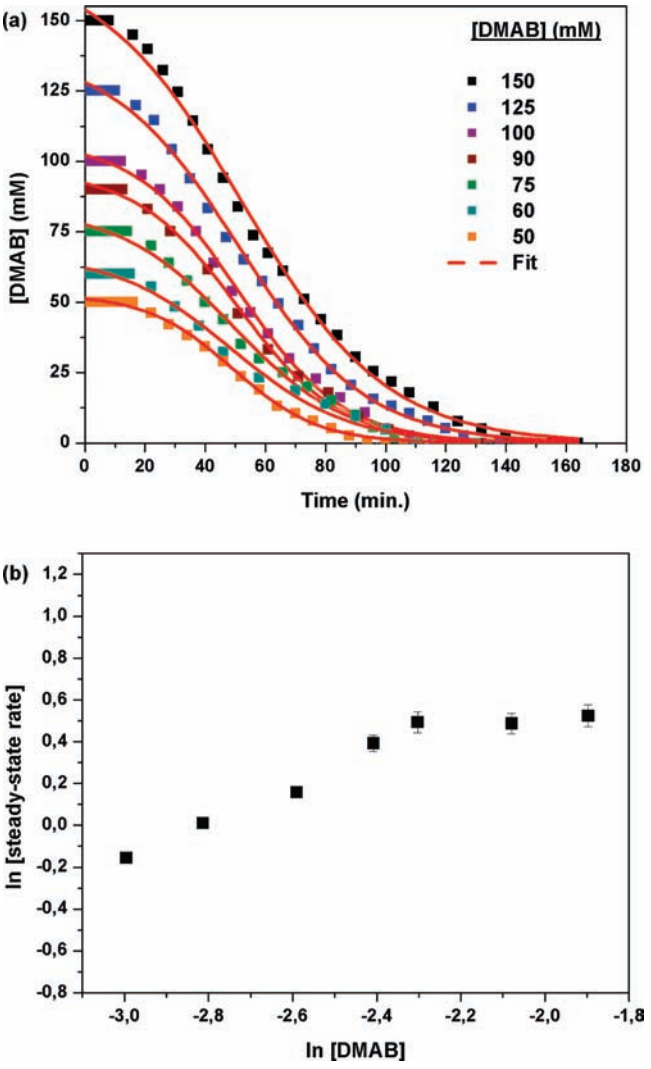

Figure 6. (a) Plots of [DMAB] loss versus time for the dehydrogenation of DMAB started with 0.10 mmol $[(C_5H_{11}CO_2)_2Rh]_2$ and various DMAB concentration at 25 ± 0.1 °C. (b) Plot of dehydrogenation rate versus [DMAB] (both in logarithmic scale) for the dehydrogenation reactions in (a).

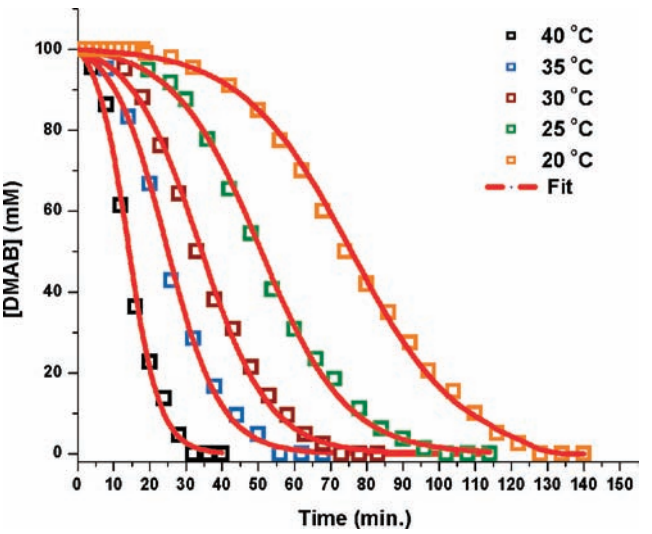

Figure 7. Plots of [DMAB] loss versus time for the dehydrogenation of DMAB started with 0.015 mmol $[(C_5H_{11}CO_2)_2Rh]_2$ and 1 mmol $Me_2NH{\bullet}BH_3$ in 10 mL toluene at various temperatures.

dehydrogenation of propane (E_a = 111 kJ/mol),[47d] the Rh(100)-catalyzed dehydrogenation of ammonia (E_a=67 kJ/mol),[47e] the Cu/C-catalyzed dehydrogenation of 2-propanol (E_a = 86 kJ/mol),[47f] the Cu/CeO_2/CNF-catalyzed dehydrogenation of 2-propanol (E_a = 41 kJ/mol),[47g] and the Y_2O_3/ZrO_2-catalyzed dehydrogenation of cyclohexanol (E_a = kJ/mol).[47h] The small value of the activation enthalpy and the large negative value of the activation entropy imply an associative mechanism in the transition state for the catalytic dehydrogenation of DMAB.[48]

All of the [DMAB] loss versus time data obtained for the catalytic dehydrogenation of DMAB under different conditions fit well to the two-step mechanism for the formation of a rhodium(0) nanocluster catalyst.[22] The rate constants k_1 and k_2 obtained from the curve fit of the data to the two-step mechanism and the k_2/k_1 ratio are given in Table 1 together with the induction period and

(48) (a) Connors, K. A. *Theory of Chemical Kinetics*; VCH Publishers: New York, 1990. (b) Twigg, M. V. *Mechanisms of Inorganic and Organometallic Reactions*; Plenum Press: New York, 1994.

Table 2. Catalyst Systems and Conditions for the Dehydrogenation of Dimethylamine−Borane[a] Tabulated from a SciFinder Literature Search of "Dimethylamine Borane Dehydrogenation"

entry	(pre)catalyst	mol % catalyst	time (h)	yield (%)	TOF (h^{-1})[b]	ref
1	[Rh (1,5-cod)(μ-Cl)]$_2$	0.5	8	100	12.4	9
2	[Ir (1,5-cod)(μ-Cl)]$_2$	0.5	136	95	0.7	9
3	$RhCl_3$	0.5	23	90	7.9	9
4	$RhCl_3 \cdot 3H_2O$	0.5	64	90	2.8	9
5	$IrCl_3$	0.5	160	25	0.3	9
6	$RhCl(PPh_3)_3$	0.5	44	95	4.3	9
7	[Cp*Rh(μ-Cl)Cl]$_2$	0.5	112	100	0.9	9
8	[Rh (1,5-cod)$_2$]OTf	0.5	8	95	12	9
9	[Rh (1,5-cod)(dmpe)]PF_6	0.5	112	95	1.7	9
10	$HRh(CO)(PPh_3)_3$	0.5	160	5	0.1	9
11	*trans*-$RuMe_2(PMe_3)_4$	0.5	16	100	12.4	9
12	*trans*-$PdCl_2(P(o\text{-tolyl})_3)_2$	0.5	160	20	0.25	9
13	Pd/C	0.5	68	95	2.8	9
14	$Rh_{colloid}$/$[Oct_4N]Cl$	2.0	6	90	8.2	11
15	Cp_2Ti[c]	2.0	4	100	12.3	13
16	$[ReBr_2(NO)(P^iPr_3)_2(CH_3CN)]$[d]	1.0	4	99	25	7
17	$[RhCl(PHCy_2)_3]$	1.0	19	100	2.63	12
18	([η^5-C_5H_3-1,3-$(SiMe_3)_2$)$_2$Ti]$_2$ (μ_2,η^1,η^1-N_2))	14	> 1	100	420	13
19	rhodium(0) nanoclusters	1.0	2.5	100	60[e]/630	this work

[a] At t = 25 °C. [b] The average TOFs were considered and calculated from the given data of corresponding reference; TOF = TON/time (h) by assuming all metal atoms are active catalysts. [c] At t = 20 °C. [d] At t = 85 °C. [e] The initial TOF value of hexanoate- and dimethylammonium-stabilized rhodium(0) nanoclusters.

the dehydrogenation rate obtained from the nearly linear portion of the curve for the catalytic dehydrogenation of DMAB under various conditions. First of all, the large value of the k_2/k_1 ratio indicates the high level of kinetic control for the formation of near-monodisperse rhodium(0) nanoclusters.[18] Although the induction period is relatively short and does not vary significantly with experimental conditions (substrate concentration, precursor concentration, and temperature), the inverse relationship between the induction time and the rate constant k_1, which has been known for a long time,[22a] is also observed in this case. When the k_1 values determined for the reaction under various conditions are plotted versus the negative logarithm of the induction period, pt(ind.) = −log[t(ind.)], one can clearly envisage their relationship. In particular, the rate constant k_1 and the induction period data for the same concentration of DMAB (100 mM, Table 1) exhibit a linear fit. However, the data points obtained for the different concentrations of DMAB deviate from linearity.

Catalyst Lifetime Experiment and Comparison of the Catalytic Activity of Dimethylammonium Hexanoate Stabilized Rhodium(0) Nanoclusters to Other Homogeneous and Heterogeneous Catalysts in the Dehydrogenation of Dimethylamine−Borane. A catalyst lifetime experiment starting with 0.005 mmol of $[(C_5H_{11}CO_2)_2Rh]_2$ and 0.05 mol of DMAB at 25 ± 0.1 °C reveals a total turnover (TTO) value of 1040 in the dehydrogenation of DMAB over 26 h before deactivation by aggregation into bulk rhodium occurs. An initial TOF value of 60 h^{-1} was obtained; however, the average TOF value was calculated to be 40 h^{-1}. The observation that the TOF value decreases as the reaction proceeds indicates the deactivation of the rhodium(0) nanocluster catalyst, evidenced also by the bulk metal precipitation at the end of the experiment. The apparent values of TTO = 1040 and TOF = 60 h^{-1} should be considered as the lower limits for the rhodium(0) nanocluster catalyst stabilized by dimethylammonium hexanoate. For the rhodium(0) nanoclusters, we know that the CS_2/total rhodium ratio is the experimentally determined 0.019 value. Although determining the exact number of metal atoms deactivated by one CS_2 molecule is difficult, a CS_2/metal stoichiometry of 1/5 can be estimated for the rhodium(0) nanoclusters based on the single-crystal data.[49] The true TTO and TOF values for rhodium(0) nanoclusters are a factor of $1/(0.019 \times 5) = 10.5$ higher than the apparent lower limit TTO of 1040 and TOF of 60 h^{-1}, which are already record values among the heterogeneous catalysts tested in this reaction. Thus, the TOF and TTO values increase to 630 h^{-1} and 10 920 turnovers of the dehydrogenation of DMAB per true active site at 25 ± 0.1 °C, respectively.

The catalytic activity of hexanoate- and dimethylammonium-stabilized rhodium(0) nanocluster catalysts is given together with the values of the previous catalysts for the same reaction in Table 2 for comparison. It is seen that the hexanoate- and dimethylammonium-stabilized rhodium(0) nanocluster catalyst is more active than the prior best heterogeneous bulk rhodium(0) metal[11] and homogeneous [η^5-C_5H_3-1,3-$(SiMe_3)_2$)$_2$Ti]$_2$ (μ_2,η^1,η^1-N_2) catalysts.[13]

Summary and Conclusions

The main findings and conclusions from this work can be summarized as follows:

(1) For the first time, dimethylammonium hexanoate stabilized rhodium(0) nanoclusters ($Rh(0)_{\sim 190}$−$Rh(0)_{\sim 460}$ nanoclusters) were reproducibly prepared from the reduction of $[(C_5H_{11}CO_2)_2Rh]_2$, during the catalytic dehydrogenation of dimethylamine−borane at room temperature.

(2) The characterization of this novel catalyst system by using TEM, STEM, EDX, XRD, XPS, FTIR, UV−vis, and ^{1}H, ^{13}C, and ^{11}B NMR spectroscopic methods as well as inductively coupled plasma optical emission spectroscopy

(49) Pandey, K. K. *Coord. Chem. Rev.* **1995**, *140*, 37.

(ICP-OES) and elemental analysis revealed the generation of 2 equiv of $[Me_2NH_2]^+[C_5H_{11}COO]^-$ per rhodium from the reduction of rhodium(II) hexanoate to rhodium(0) nanoclusters. The hexanoate anions and dimethylammonium cations take part in stabilization of the rhodium(0) nanoclusters.

(3) The dimethylammonium hexanoate stabilized rhodium(0) nanoclusters show unprecedented catalytic activity among the heterogeneous catalysts tested in the dehydrogenation of DMAB at 25 °C and provide complete conversion of $Me_2NH \cdot BH_3$ to $[Me_2NBH_2]_2$ plus 2 equiv of H_2 gas released, with a TOF of 60 h^{-1} and a TTO of 1040 mol of H_2 per mol of Rh.

(4) The quantitative kinetic studies depending on the catalyst concentration, substrate concentration, and temperature reveal that the rhodium(0) nanocluster catalyzed dehydrogenation of DMAB is first-order in the rhodium concentration. With respect to the substrate concentration, it appears to be zero-order when [DMAB] > 90 mM and first-order at lower concentration. For the first time, the activation parameters became available for the catalytic dehydrogenation of dimethylamine−borane. The small values of the activation energy and enthalpy (E_a = 34 kJ/mol; $\Delta H^{\ddagger}$ = 34.5 kJ/mol) and the large negative value of the activation entropy ($\Delta S^{\ddagger} = -133$ J/mol·K) are indicative of an associative mechanism in the transition state for the catalytic dehydrogenation of dimethylamine−borane.

(5) All of the kinetic data, collected for the nanocluster formation and concomitant dehydrogenation of DMAB catalyzed by dimethylammonium hexanoate stabilized rhodium(0) nanoclusters under various experimental conditions, fit well to the two-step mechanism for the nanocluster formation:[22] nucleation (A → B, rate constant k_1) and then autocatalytic surface growth (A + B → 2B, rate constant k_2). The large value of the k_2/k_1 ratio is indicative of the high level of kinetic control in the formation of rhodium(0) nanoclusters from reduction of the soluble precursor rhodium(II) hexanoate.

(6) Employment of the methodology developed by Finke et al.[50] delivered additional useful results. UV−vis and TEM studies, mercury(0)/CS_2 poisoning, and nanofiltration experiments provide compelling evidence that rhodium(0) nanoclusters formed from the reduction of rhodium(II) hexanoate are the true heterogeneous catalyst in the dehydrogenation of DMAB. In that sense, this is really the first report on the transition-metal nanoclusters catalyzed dehydrogenation of DMAB.

(7) The reporter reaction method developed by Finke et al.[51] for the catalytic hydrogenation of olefins and aromatics was shown to work also in the case of rhodium(0) nanocluster formation from the reduction of rhodium(II) hexanoate during the catalytic dehydrogenation reaction of DMAB. Monitoring the hydrogen evolution in the dehydrogenation of DMAB provides an indirect route to follow the nucleation and autocatalytic surface growth of metal(0) nanoclusters from the reduction of a soluble precursor in an organic solvent. After the known cyclohexene hydrogenation, the dehydrogenation of DMAB is the second reporter reaction for the nanocluster formation kinetics.

Acknowledgment. Partial support by the National Boron Research Institute (Project 2008-C-0146) and the Turkish Academy of Sciences is acknowledged.

Supporting Information Available: Experimental section, photographs of the reaction solution in the course of dehydrogenation of DMAB and corresponding UV−vis spectra (Figure S1), STEM image and STEM-EDX spectrum of hexanoate- and dimethylammonium-stabilized rhodium(0) nanoclusters (Figure S2), plot of the relative rate versus molar ratio of CS_2/total rhodium for CS_2 poisoning of rhodium(0) nanoclusters during dehydrogenation of DMAB (Figure S3), ^{11}B NMR spectra of DMAB and the reaction solution at the end of dehydrogenation (Figure S4), powder XRD pattern of isolated and vacuum-dried rhodium(0) nanoclusters (Figure S5), Rh 3d XPS spectrum and its simulated peak fitting for the isolated and vacuum-dried samples of rhodium(0) nanoclusters (Figure S6), FTIR spectrum of isolated and vacuum-dried samples of rhodium(0) nanoclusters (Figure S7), ^{13}C NMR of the neat reaction mixture from the catalytic dehydrogenation of DMAB (Figure S8), plot of the dehydrogenation rate versus rhodium concentration (both on log scale) for the catalytic dehydrogenation of DMAB at 25 ± 0.1 °C (Figure S9), (a) $\ln(k_{obs})$ vs $1/T$ graph (Arrhenius plot), (b) $\ln(k_{obs}/T)$ vs $1/T$ graph (Eyring plot) for the dimethylammonium hexanoate stabilized rhodium(0) nanocluster catalyzed dehydrogenation of DMAB (Figure S10), and plot of k_1 (min^{-1}) vs pt (pt = $-\log t$(ind.); Figure S11). This material is available free of charge via the Internet at http://pubs.acs.org.

(50) Lin, Y.; Finke, R. G. *Inorg. Chem.* **1994**, *33*, 4891.

(51) Lin, Y.; Finke, R. G. *J. Am. Chem. Soc.* **1994**, *116*, 8335.